Surveying the repair of ancient DNA from bones via high-throughput sequencing

Nathalie Mouttham[1,2], Jennifer Klunk[1,2], Melanie Kuch[1], Ron Fourney[3], and Hendrik Poinar[1,2,4]
[1] McMaster Ancient DNA Centre, Department of Anthropology, McMaster University, Hamilton, ON, Canada, [2] Department of Biology, McMaster University, Hamilton, ON, Canada, [3] Science and Strategic Partnerships, Forensic Science and Identification Services, Royal Canadian Mounted Police, Ottawa, ON, Canada, and [4] Michael G. DeGroote Institute for Infectious Disease Research, McMaster University, Hamilton, ON, Canada

BioTechniques 59:19-25 (July 2015) doi 10.2144/000114307
Keywords: ancient DNA; DNA damage; DNA repair; high-throughput sequencing

Supplementary material for this article is available at www.BioTechniques.com/article/114307.

DNA damage in the form of abasic sites, chemically altered nucleotides, and strand fragmentation is the foremost limitation in obtaining genetic information from many ancient samples. Upon cell death, DNA continues to endure various chemical attacks such as hydrolysis and oxidation, but repair pathways found in vivo no longer operate. By incubating degraded DNA with specific enzyme combinations adopted from these pathways, it is possible to reverse some of the post-mortem nucleic acid damage prior to downstream analyses such as library preparation, targeted enrichment, and high-throughput sequencing. Here, we evaluate the performance of two available repair protocols on previously characterized DNA extracts from four mammoths. Both methods use endonucleases and glycosylases along with a DNA polymerase-ligase combination. PreCR Repair Mix increases the number of molecules converted to sequencing libraries, leading to an increase in endogenous content and a decrease in cytosine-to-thymine transitions due to cytosine deamination. However, the effects of Nelson Repair Mix on repair of DNA damage remain inconclusive.

Ancient DNA (aDNA) is defined as DNA extracted from archival, archeological, forensic, or paleontological specimens (1). It is typically highly degraded as a result of having withstood chemical and physical assaults from post-mortem enzymatic digestion and environmental degradation (2,3). Common characteristics of an aDNA extract include: short fragment lengths (typically <150 bp) due to extensive fragmentation; single-stranded termini DNA where the majority of base damage is located (4); low endogenous (or target) DNA content (i.e., mammoth DNA, in this case), though this can be variable (5,6); high exogenous (or non-target) ancient DNA content, most often comprised of bacteria from the specimen's microbiome and environment at the time of death; and in some cases, better preserved DNA from modern contamination. It is expected that the damaged DNA in both the endogenous and exogenous fractions will have similar degradation patterns due to similar preservation conditions.

Although more contemporary DNA, which could still be centuries old, will likely have longer fragments and fewer intrinsic damaged sites, the age of a sample has little correlation with the extent of DNA degradation. Many factors, such as the specimen's preservation conditions or the time until burial, are more reliable predictors of long-term DNA preservation (7). Most ancient samples no longer contain enough DNA to be quantifiable by traditional methods, but the field of aDNA has circumvented this issue by finding innovative ways of exploiting genomic methodologies, such as the analysis of extremely short fragments via high-throughput sequencing (HTS) (8).

Types of typical aDNA damage are summarized in Supplementary Table S1, but the following three should be highlighted: Apurinic and apyrimidinic sites (AP sites) result from the cleavage of the β-N-glycosidic bond between the base and the deoxyribose (3). They occur more frequently in deoxyguanosine or deoxyadenosine, due to a weak carbon-purine bond (9), and they can prevent

METHOD SUMMARY

Active and heat-inactivated enzymatic DNA repair with the PreCR and Nelson protocols was performed on four mammoth extracts (each in technical duplicates) and one mylodon blank. Repaired extracts were placed into indexed libraries and high-throughput sequenced. The repair efficiency of each method was evaluated based on mitochondrial and nuclear endogenous contents, fragment length distributions, and base misincorporation counts, which were established from 3-million-read subsets of each library.

Table 1. Summary of all enzymes used in Nelson and PreCR repair protocols.

Enzyme	Nelson	PreCR	Substrate	Function
Endonuclease IV	✓	✓	AP sites in ssDNA or dsDNA	Cleaves phosphodiester bond at 5′ of AP site; removes unsaturated aldehyde and phosphate from 3′ termini; leaves 5′ deoxyribose-5-phosphate and 3′ hydroxyl groups
T4 Pyrimidine-dimer-glycosylase (T4 PDG)	✓	✓	cis-syn-cyclobutane pyrimidine dimers	Cleaves N-glycosydic bond at 5′ end of dimer to create AP site; removes one thymine from dimer (second thymine remains as first base at 3′ end of AP site)
Endonuclease VIII	✓	✓	Damaged pyrimidines in dsDNA	Cleaves N-glycosydic bond at 5′ end of damaged base to create AP site; cleaves at 5′ and 3′ end of AP site to create 3′ phosphate (via 3′ α,β-unsaturated aldehyde) and 5′ phosphate termini, respectively
Formaminidopyrimidine-DNA-glycosylase (FPG)	✓	✓	Damaged purines in ssDNA or dsDNA	Cleaves N-glycosydic bond at 5′ end of damaged base to create AP site; cleaves at 5′ and 3′ end of AP site to create 3′ phosphate (via 3′ α,β-unsaturated aldehyde) and 5′ phosphate termini, respectively
***Taq* ligase**		✓	dsDNA	Catalyzes formation of phosphodiester bond between juxtaposed 5′ phosphate and 3′ hydroxyl termini in dsDNA; cannot repair ss nicks; activity less optimal at 37°C
T4 ligase	✓		dsDNA	Catalyzes formation of phosphodiester bond between juxtaposed 5′ phosphate and 3′ hydroxyl termini in dsDNA; can repair ss nicks in dsDNA
***Bst* DNA polymerase**		✓	dsDNA	DNA polymerase with 5′-3′ exonuclease nick translation; no 3′-5′ exonuclease proof-reading; no strand displacement
***E.coli* DNA polymerase I**	✓		dsDNA	DNA polymerase with 3′-5′ exonuclease proof-reading activity and 5′-3′ exonuclease nick translation; requires 3′ hydroxyl termini and dsDNA template; cannot translate nicks with 5′ deoxyribose-5-phosphate termini
Uracil-DNA- glycosylase (UDG)		✓	Deaminated cytosines in ssDNA or dsDNA	Cleaves N-glycosydic bond of uracil to create AP site

AP site: apurinic or apyrimidinic site; ssDNA: single-stranded DNA; dsDNA: double-stranded DNA.

extension during replication by stalling DNA polymerases. As such, while longer, damaged fragments may be preserved, there will be an amplification bias toward shorter undamaged or less-damaged DNA templates. Many nucleotide repair enzymes require an AP intermediate. If they are not removed by endonuclease IV, new abasic sites can be created during enzymatic repair, artificially increasing the level of pre-existing DNA damage. Additionally, single-stranded nicks (ss nicks) in double-stranded DNA (dsDNA) due to breaks in the phosphodiester bond of the deoxyribose backbone are prevalent (3) and require the presence of the complementary strand to be repaired. Lastly, the conversion of deaminated cytosines to uracil bases, normally not found in DNA, is caused by the loss of an amine group. Cytosine deamination is a common occurrence in ancient extracts (2): it occurs naturally over time and persists after the death of an organism. As ubiquitous as they are, deaminated cytosines have a lesser overall impact in terms of sequence retrieval, as they induce miscoding lesions in the DNA sequence, without preventing amplification or hindering library preparation. However, as many researchers in the field perform uracil removal in pre-library preparation, which results in the loss of short-terminal sequences, the presence of deaminated cytosines can affect the recovery of sequence data from fossil remains. Since they can be observed in the sequencing data, their patterns can be used for authenticating ancient DNA (4).

DNA damage occurs in every living organism and is used as a measure of stress or aging (10). There are *in-vivo* repair mechanisms (e.g., nucleotide or base excision repair pathways) to counteract this perpetual deterioration (11). These repair pathways are efficient and usually accurate, though some damaged bases can occasionally be omitted, leading to mutations. Upon death, however, DNA continues to face hydrolytic, oxidative and UV attacks that are not repaired post-mortem. This subsequent damage, commonly observed in ancient and forensic samples, is the single most important limitation to retrieving genetic information from deceased organisms. By using enzymatic mixtures very close to those found in the excision repair pathways, some DNA damage may theoretically be reversed.

The efficacy of two in vitro repair protocols was evaluated using ancient mammoth DNA extracts previously characterized by a targeted qPCR assay (12) (see Supplementary Table S2 for details). Table 1 summarizes the enzymatic composition of both kits. The first one is the commercially available PreCR Repair Mix from New England Biolabs (Ipswich, MA). This kit has been previously tested for forensic applications (13–15). However, these evaluations focused on short tandem repeat (STR) profiling, whereas this project, like the majority of current aDNA projects, is HTS-based. The second enzymatic mixture was obtained from a U.S. Department of Justice report, titled "Repair of damaged DNA for forensic analysis" (J. Nelson, 2009). It was chosen because of its similarities to the PreCR Repair Mix: they each have four common endonuclease/glycosylases but have different ligase-DNA polymerase combinations, and PreCR also contains a uracil-DNA-glycosylase.

Materials and methods

More detailed descriptions of the materials and methods can be found in the Supplementary Material.

Experimental design

When deciding on controls for repair efficacy, active repair reactions could be compared with (*i*) non-repaired extracts or (*ii*) heat-inactivated repair reactions, and the latter were selected. The heat-inactivated controls were critical in establishing which changes to aDNA extracts were caused by non-enzymatic reactions due to pH, ionic concentration, or buffer components. As such, the results presented are a comparison of heat-inactivated and active enzymatic repair mixtures.

Two additional types of negative controls were used in this study: extraction and carrier blanks. Extraction (or reagent) blanks undergo the same process as the normal samples but do not contain any DNA, allowing for the detection of contamination introduced by reagents. Carrier blanks play the same role as extraction blanks, except they contain DNA from another ancient sample (*Mylodon darwinii,* an extinct ground sloth). This type of control, sometimes found in aDNA studies, favors the detection of minute amounts of cross-contaminating DNA by creating a carrier effect via an artificial exogenous background (16).

Sample choice and DNA extraction

DNA was extracted from technical duplicates of four mammoth (genus *Mammuthus*) specimens, chosen for their varying endogenous contents, and one mylodon specimen used as a carrier blank. Multiple 100–200 mg subsamples of bone were demineralized and digested. DNA was obtained using a modified proteinase K digestion and subsequent phenol-chloroform-isoamyl alcohol extraction method (17,18).

DNA repair

PreCR Rpair Mix was prepared in 30 µL, according to the manufacturer's instructions (New England Biolabs), and Nelson Repair Mix was prepared in 30 µL, according to the author's instructions. Heat-inactivated reactions mixes were incubated at 95°C (PreCR) or 85°C (Nelson) for 20 min while the active mixtures were kept on ice. Aliquots of ~50 ng total DNA were added and reactions were incubated at 37°C for 20 min. To inactivate the reaction, repaired extracts were purified over a MinElute column, following the manufacturer's instructions (Qiagen, Venlo, The Netherlands).

Library preparation and quantification

The protocol followed is a modified version of Meyer & Kircher (19), with the modifications described in Kircher et al. (20) for double-indexing. A quantification assay targeting the cluster generation sequence was performed, which measured the number of adapted molecules. Based on these values, each sample was normalized to the number of copies in 1 µl of the lowest, non-extraction blank sample and was pooled at an equal copy number.

Sequencing and data curation

All sequencing was performed using a rapid flow cell on a HiSeq 1500

(Illumina, San Diego, CA), using a 2 × 100 bp HiSeq Reagent Kit according to the manufacturer's recommendations. Raw data were processed with HiSeq Control Software (HCS) (Illumina) v1.5.15.1 and Real-Time Analysis (RTA) (Illumina) v1.13.48.0. File conversion and demultiplexing using each 7-bp reverse index (requiring a 100% match) were performed using CASAVA (Illumina) v1.8.2.

Sequencing data were curated and aligned, based on the parameters in Enk et al. (21), using cutadapt v.1.2 (22), FLASH v.1.0.3 (23), and Burrows-Wheeler Aligner v.0.6.1-r104 (BWA) (24). The mammoth (*Mammuthus primigenius*) mitochondrial genome (GenBank Accession No. JF912200.1) (25) and the masked repeat nuclear African elephant (*Loxodonta africana*) consensus genome (Loxafr3.0 from the Broad Institute, RefSeq Assembly ID: GCF_000001905.1) were used as references. Random 3 million read subsets of all reads at least 24 bp long (26) were taken from each library to analyze endogenous content, fragment length distribution, and base misincorporations using mapDamage v.2.0 (27). A paired, two-sample *t*-test ($\alpha = 0.05$) was used to determine statistical significance for all analyses. Reads were uploaded to the Short Read Archive (Project Number PRJNA276848).

Table 2. Summary of the differences observed between inactive and active Nelson and PreCR enzymatic repair mixtures.

	Figure	Nelson		PreCR	
		Trend	*p*-value	Trend	*p*-value
Number of adapted molecules	S1	↘	0.03	No trend	0.16
Endogenous mitochondrial content	1	↘	<0.01	↗	<0.01
Endogenous nuclear content	1	↘	0.06	↗	0.01
Total reads median length	2	↗	<0.01	↘	0.09
Mitochondrial reads median length	2	↗	0.16	↘	0.10
Nuclear reads median length	2	↗	0.91	↘	0.02
Number of C to T misincorporations	3	↗	0.21	↘	<0.01
Number of G to T misincorporations	3	No trend	0.53	↘	0.12

↗: increase, ↘: decrease; red: statistically significant, S: Supplementary figure. The overall trends and associated *p*-values from a paired, two-tailed *t*-test ($\alpha = 0.05$) were calculated from the mean of all samples available.

Results and discussion

A summary and interpretation of the results is presented in Table 2. It is clear that both the active Nelson and PreCR reaction mixtures have distinct effects on ancient extracts, based on endogenous DNA content, fragment length distributions, and base misincorporations. The selected mammoth specimens come from bones preserved in permafrost regions and, as such, should not be seen as representative of all ancient DNA samples. However, they do offer a more realistic model of DNA degradation than artificially damaged samples, and the subsequent conclusions can likely be extrapolated and extended to other types of sample tissues and preservation conditions.

Quantitative PCR measurements targeted to the 5′ end of each index show that, given the same library preparation DNA input, there was no significant variation in adaptation or indexing, as the number of adapted molecules is within the same order of magnitude for all extracts (Supplementary Figure S1).

Endogenous mitochondrial and nuclear contents were calculated based on the number of reads that mapped to the mammoth mitochondrial genome and a masked repeat African elephant nuclear reference genome (Figure 1). Not surprisingly, only 0.008%–0.05% (~190–1400 reads) of the total fragments map to the *M. primigenius* mitochondrial genome. Conversely, the nuclear endogenous content is higher,

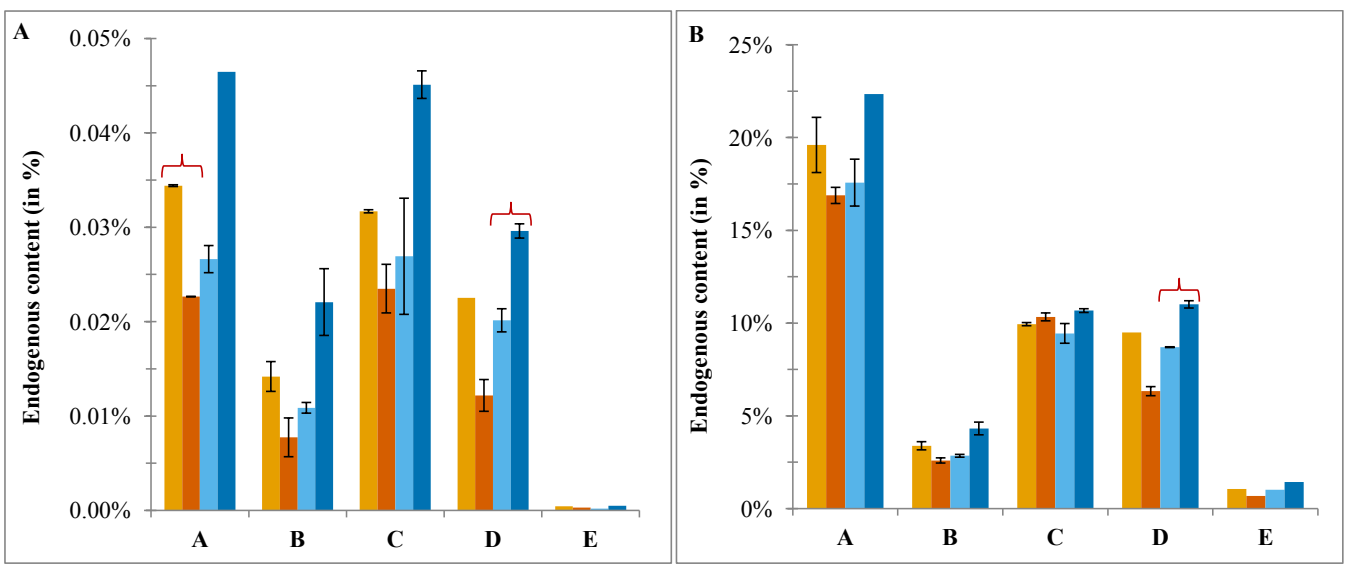

Figure 1. Endogenous mitochondrial and nuclear content of four mammoth samples and one mylodon blank after undergoing active or heat-inactivated DNA repair with the Nelson or PreCR protocols. Four mammoth extracts (A-D) and one mylodon carrier blank (E) were incubated with active or heat-inactivated DNA enzymatic repair mixtures, either Nelson (in dark and light orange, respectively) or PreCR (in dark and light blue, respectively). Reads from repaired extracts were mapped to the mitochondrial (panel A) and nuclear (panel B) reference genomes. Values are expressed as a percentage of the total number of reads available for each extract and were calculated as the mean of two technical replicates; error bars show one standard deviation (when available). Statistically significant variations are marked with a red bracket.

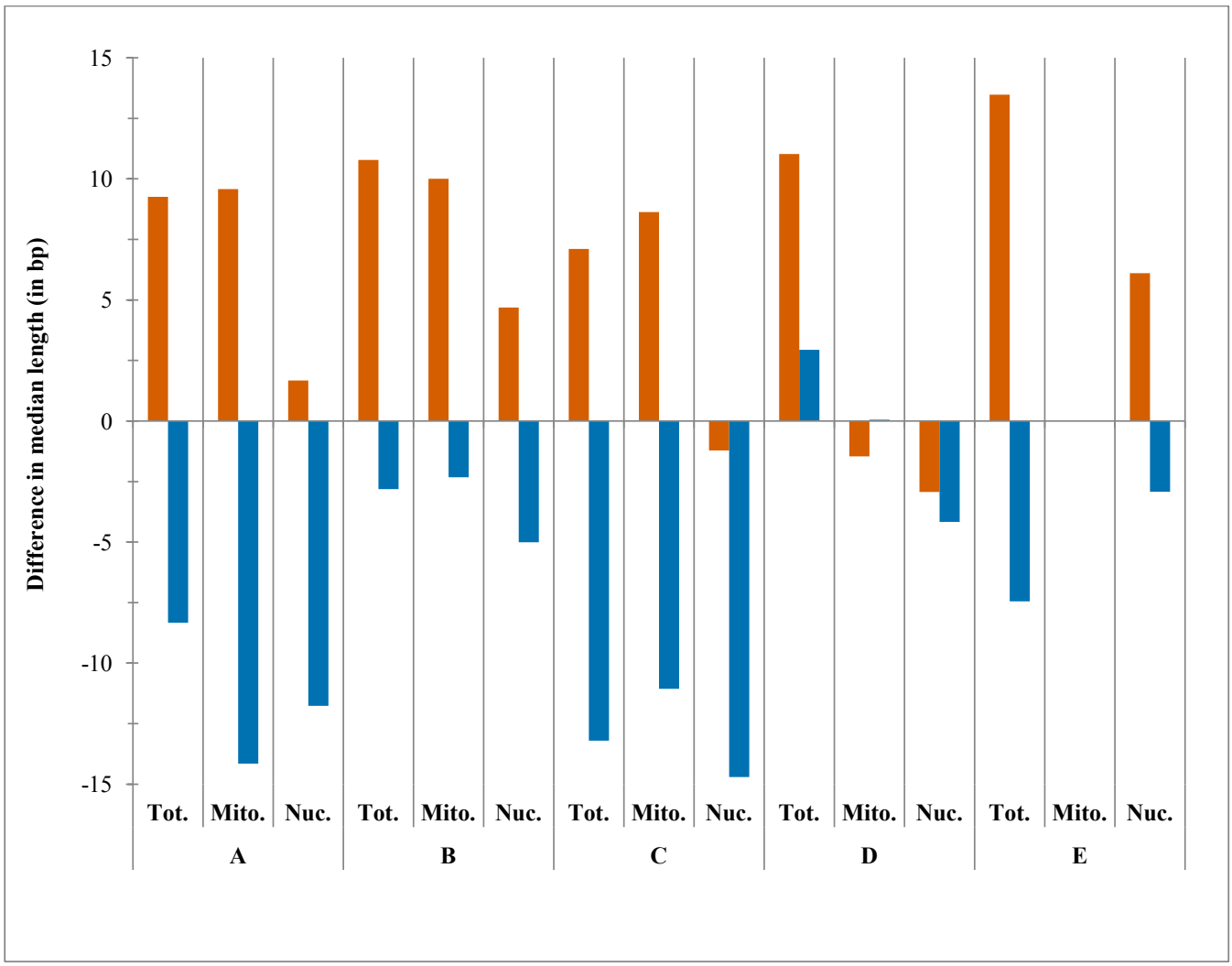

Figure 2. Differences in median fragment length of the total, mitochondrial, and nuclear content of four mammoth samples and one mylodon blank between heat-inactivated and active DNA repair mixtures from the Nelson or PreCR protocols. Four mammoth extracts (samples A-D) and one mylodon blank (sample E) were incubated with Nelson (in orange) or PreCR (in blue) enzymatic repair mixtures. Median fragment length for total (Tot.), mitochondrial (Mito.), and nuclear (Nuc.) reads were calculated. The values for each median length can be inferred from the dashed lines of Supplementary Figures S2 and S3.

representing almost 25% of the reads (~620,000 reads) for sample A and as low as 2.5% (~75,000 reads) for sample B. This heterogeneity is characteristic of the diversity seen in most aDNA specimens. The extraction (reagent) blanks yielded a negligible amount of total sequencing reads (~300–43,000 reads) (data not shown) or nuclear mammoth reads (<15 reads) (data not shown). A 49-bp quantitative PCR assay targeting the mitochondrial mammoth genome performed after the enzymatic repair reactions confirmed the presence of negligible amounts of mammoth reads in the carrier and extraction blanks (<3 copies per μl) (data not shown).

There is an increase in the proportion of shorter fragments from total reads (Supplementary Figure S2) and from mapped nuclear reads (Supplementary Figure S3) in active PreCR Repair Mix compared with the heat-inactivated mix. Likewise, the average decrease in median fragment length seen in total DNA reads (-5.79 bp) is accentuated in mitochondrial (-6.60 bp) and nuclear (-7.52 bp) mammoth reads (Figure 2), implying that length reduction is occurring preferentially in degraded molecules and presumably in the fragile single-stranded termini. Given the number of sequential enzymatic activities that need to take place to repair heavily degraded DNA molecules, it is probable that additional AP sites and ss nicks are formed during the repair process.

A successful enzymatic repair should be marked by an increase in overall fragment length (i.e., previously unavailable longer fragments become accessible), and an increase in the number of adapted molecules or total overall content (i.e., more reads are mapped to the reference genome). However, the exact opposite is seen in Figure 1 and Table 2, and corroborated by Supplementary Figure S3: the endogenous DNA content decreases post-Nelson repair protocol. This would imply that the reaction is increasing the fragment length of total reads while simultaneously decreasing the number of endogenous fragments. Note that no overall conclusion can be made about the length of endogenous reads,

as there is too much variability among the samples. From these contradictory statements, it is clear that no easily discernible repair is taking place.

A qualitative assessment of the DNA post-repair reactions was established by mapping reads against the *M. primigenius* mitochondrial genome using mapDamage2.0 and counting the base misincorporations (i.e., substitutions, insertions, and deletions) observed (see Supplementary Table S3 for all values). Cytosine (C) to thymine (T) misincorporations, which are the result of cytosine deamination, are repaired by uracil-DNA-glycosylase (UDG) (Figure 3A). The absence of UDG from the Nelson Repair Mix accounts for the similarities seen between active and inactive reactions. The decrease in number of C to T misincorporations in active compared with inactive PreCR Repair Mix is significant in most samples (statistics could not be calculated for sample A due to a failed technical replicate). The data suggest at a minimum that UDG is functioning properly in the repair reaction. Guanine (G) to T misincorporations are representative of guanine oxidation (leading to thymine glycol) and are repaired by formaminidopyrimidine-DNA-glycosylase (FPG) (Figure 3B). For both active Nelson and PreCR repair mixtures, the high variation and lack of clear trend in G to T mutations indicate that the activity of FPG is either hindered, highly variable, or the damage is not frequent enough to notice clear trends in repair. FPG favors dsDNA as a substrate in order to repair oxidized purines, and this may be a limiting factor in its efficacy in aDNA extracts, which tend to contain many single-stranded overhangs. This observation would apply to any enzyme with the same dsDNA substrate requirement.

Given these results, it appears that most of the trends observed for PreCR Repair Mix stem from UDG activity. It is the only enzyme that can repair the damage-prone 10–15 bp single-stranded fragment termini common in aDNA. UDG cleaves off uracil but leaves behind an unrepaired AP site that is likely cleaved (and thus the termini are lost) by the action of endonuclease IV. This decreases the length of all fragments but affects the ancient endogenous content more readily than the modern exogenous content (Figure 2). As the phospodiester backbone of unrepaired AP sites eventually breaks, the remaining ssDNA stretch would likely be lost prior to library preparation. Whether this accounts for the increase in adapted molecules (Supplementary Figure S1) and endogenous DNA content (Figure 1) is unclear. The results presented here are consistent with previous STR-based evaluations, where peak height decrease or allelic drop-out was observed in more complex DNA samples equivalent to aDNA specimens (14,15).

The interpretation of the Nelson Repair Mix data is less straightforward. Since the Nelson Repair Mix does not contain UDG, the enzymes can only repair damaged bases in dsDNA. Endonuclease IV creates 5′ deoxyribose-5-phosphate termini when it repairs AP sites. Consequently, DNA polymerase I is unable to translate nicks due to AP site cleavage, unlike *Bst* polymerase in the PreCR Repair Mix. Unrepaired AP sites can lead to blunt-end double-stranded breaks. This artificial degradation is more likely to occur on previously damaged fragments and as such, the endogenous fraction is more likely than the more recent exogenous components to acquire damage. The repaired fragments are then likely too damaged to be converted into sequencing libraries or are below the 24-bp mapping cutoff used here. As such, the increase in total fragment length is simply an artifact of the decrease in short, degraded reads, both endogenous and exogenous. This explanation may account for the decrease in overall endogenous content (Figure 1), the statistically significant increase in read length, and the inconclusive increase in endogenous fragment length (Figure 2). Alternatively, since T4 ligase in the Nelson Repair Mix is more efficient at binding blunt-end fragments together than *Taq* ligase in PreCR, we hypothesize that active Nelson Repair Mix ligates random blunt-end fragments together, creating hybrids that may have problems mapping

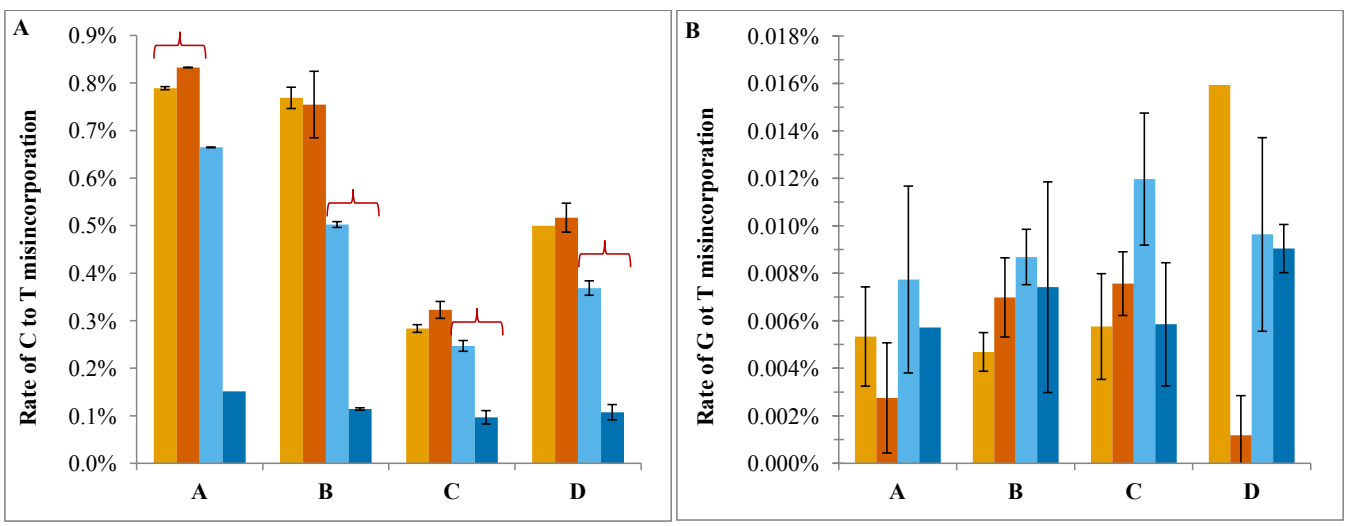

Figure 3. Occurrence of base misincorporation in mitochondrial reads from four mammoth samples after undergoing active or heat-inactivated DNA repair with the Nelson or PreCR protocols. Four mammoth extracts (A-D) were incubated with active or heat-inactivated DNA enzymatic repair mixtures, either Nelson (in dark and light orange, respectively) or PreCR (in dark and light blue, respectively). Two types of misincorporation were counted: transition of cytosine (C) to thymine (T) (panel A) and transition of guanine (G) to T (panel B). Values are expressed as a percentage of the total number of bases that mapped to the mitochondrial genome and were calculated as the mean of two technical replicates; error bars show one standard deviation. Statistically significant variations are marked with a red bracket.

to the reference genome and causing a decrease in the endogenous content (not tested in this paper).

Repairing damaged DNA could have useful applications in many other fields. While the idea of having multiple repair enzymes in a one-step reaction remains attractive for large-scale applications that require robust reproducibility and consistency, it is advised that sequential repair protocols, where one enzymatic reaction is performed at a time, should be explored for optimal DNA repair of ancient extracts (28).

In conclusion, under the conditions outlined above, there does not appear to be appreciable repair of ancient mammoth bone DNA. The repair of ancient DNA extracts with PreCR Repair Mix yields overall shorter DNA fragments and fewer numbers of base misincorporations by virtue of removal of deaminated cytosines via UDG. The efficiency of the other enzymatic components could not be clearly measured, and thus, it is difficult to assess their efficacy during the PreCR repair protocol. DNA repair with the Nelson protocol shows inconclusive results and cannot be recommended at this point until further analyses have been performed. Optimizing enzymatic repair will be critical for the genetic analysis of previously unattainable samples, including heavily damaged fossil DNA extracts, forensic biological evidence, and medical bio-bank specimens.

Author contributions

N.M., M.K., and H.P. designed the experiments and performed analyses. J.K. performed the sequencing data curation. N.M. carried out the experiments and prepared the manuscript. All authors edited the manuscript.

Acknowledgments

We thank current and former members of the McMaster Ancient DNA Centre for their invaluable guidance and input throughout this entire project. Comments from Lara Moutthamand each reviewer greatly improved this manuscript. H.P. was supported by a Canada Research Chair in Paleogenetics and McMaster University. This research was funded by the Canadian Police Research Center 02-3027.

Competing interests

The authors declare no competing interests.

References

1. **Capelli, C., F. Tschentscher, and V.L. Pascali.** 2003. "Ancient" protocols for the crime scene? Similarities and differences between forensic genetics and ancient DNA analysis. Forensic Sci. Int. *131*:59-64.
2. **Pääbo, S.** 1989. Ancient DNA: extraction, characterization, molecular cloning, and enzymatic amplification. Proc. Natl. Acad. Sci. USA *86*:1939-1943.
3. **Lindahl, T.** 1993. Instability and Decay of the Primary Structure of DNA. Nature *362*:709-715.
4. **Briggs, A.W., U. Stenzel, P.L. Johnson, R.E. Green, J. Kelso, K. Prufer, M. Meyer, J. Krause, et al.** 2007. Patterns of damage in genomic DNA sequences from a Neandertal. Proc. Natl. Acad. Sci. USA *104*:14616-14621.
5. **Green, R.E., J. Krause, S.E. Ptak, A.W. Briggs, M.T. Ronan, J.F. Simons, L. Du, M. Egholm, et al.** 2006. Analysis of one million base pairs of Neanderthal DNA. Nature *444*:330-336.
6. **Meyer, M., M. Kircher, M.T. Gansauge, H. Li, F. Racimo, S. Mallick, J.G. Schraiber, F. Jay, et al.** 2012. A high-coverage genome sequence from an archaic Denisovan individual. Science *338*:222-226.
7. **Pääbo, S., H. Poinar, D. Serre, V. Jaenicke-Despres, J. Hebler, N. Rohland, M. Kuch, J. Krause, et al.** 2004. Genetic analyses from ancient DNA. Annu. Rev. Genet. *38*:645-679.
8. **Dabney, J., M. Knapp, I. Glocke, M.T. Gansauge, A. Weihmann, B. Nickel, C. Valdiosera, N. Garcia, et al.** 2013. Complete mitochondrial genome sequence of a Middle Pleistocene cave bear reconstructed from ultrashort DNA fragments. Proc. Natl. Acad. Sci. USA *110*:15758-15763.
9. **Olafsson, P.G., A.M. Bryan, G.C. Davis, and S. Anderson.** 1974. A comparative study of the relative ease of thermolytic depurination vs. depyrimidination in 2'-deoxynucleosides. Can. J. Biochem. *52*:997-1002.
10. **Ames, B.N.** 1989. Endogenous DNA damage as related to cancer and aging. Mutat. Res. *214*:41-46.
11. **Frosina, G., P. Fortini, O. Rossi, F. Carrozzino, G. Raspaglio, L.S. Cox, D.P. Lane, A. Abbondandolo, and E. Dogliotti.** 1996. Two pathways for base excision repair in mammalian cells. J. Biol. Chem. *271*:9573-9578.
12. **Debruyne, R., G. Chu, C.E. King, K. Bos, M. Kuch, C. Schwarz, P. Szpak, D.R. Grocke, et al.** 2008. Out of America: ancient DNA evidence for a new world origin of late quaternary woolly mammoths. Curr. Biol. *18*:1320-1326.
13. **Diegoli, T.M., M. Farr, C. Cromartie, M.D. Coble, and T.W. Bille.** 2012. An optimized protocol for forensic application of the PreCR Repair Mix to multiplex STR amplification of UV-damaged DNA. Forensic Sci. Int. Genet. *6*:498-503.
14. **Robertson, J.M., S.M. Dineen, K.A. Scott, J. Lucyshyn, M. Saeed, D.L. Murphy, A.J. Schweighardt, and K.A. Meiklejohn.** 2014. Assessing PreCR repair enzymes for restoration of STR profiles from artificially degraded DNA for human identification. Forensic Sci. Int. Genet. *12*:168-180.
15. **Ambers, A., M. Turnbough, R. Benjamin, J. King, and B. Budowle.** 2014. Assessment of the role of DNA repair in damaged forensic samples. Int J Legal Med. *128*:913-921.
16. **Xu, Z., F. Zhang, B. Xu, J. Tan, S. Li, and L. Jin.** 2009. Improving the sensitivity of negative controls in ancient DNA extractions. Electrophoresis *30*:1282-1285.
17. **Schwarz, C., R. Debruyne, M. Kuch, E. McNally, H. Schwarcz, A.D. Aubrey, J. Bada, and H. Poinar.** 2009. New insights from old bones: DNA preservation and degradation in permafrost preserved mammoth remains. Nucleic Acids Res. *37*:3215-3229.
18. **Poinar, H.N., C. Schwarz, J. Qi, B. Shapiro, R.D. Macphee, B. Buigues, A. Tikhonov, D.H. Huson, et al.** 2006. Metagenomics to paleogenomics: large-scale sequencing of mammoth DNA. Science *311*:392-394.
19. **Meyer, M. and M. Kircher.** 2010. Illumina sequencing library preparation for highly multiplexed target capture and sequencing. Cold Spring Harb Protoc *2010*:pdb prot5448.
20. **Kircher, M., S. Sawyer, and M. Meyer.** 2012. Double indexing overcomes inaccuracies in multiplex sequencing on the Illumina platform. Nucleic Acids Res. *40*:e3.
21. **Enk, J., J.M. Rouillard, and H. Poinar.** 2013. Quantitative PCR as a predictor of aligned ancient DNA read counts following targeted enrichment. Biotechniques *55*:300-309.
22. **Martin, M.** 2011. Cutadapt removes adapter sequences from high-throughput sequencing reads. EMBnet.journal *17*:10-12.
23. **Magoc, T. and S.L. Salzberg.** 2011. FLASH: fast length adjustment of short reads to improve genome assemblies. Bioinformatics *27*:2957-2963.
24. **Li, H. and R. Durbin.** 2009. Fast and accurate short read alignment with Burrows-Wheeler transform. Bioinformatics *25*:1754-1760.
25. **Enk, J., A. Devault, R. Debruyne, C.E. King, T. Treangen, D. O'Rourke, S.L. Salzberg, D. Fisher, et al.** 2011. Complete Columbian mammoth mitogenome suggests interbreeding with woolly mammoths. Genome Biol. *12*:R51.
26. **Sawyer, S., J. Krause, K. Guschanski, V. Savolainen, and S. Paabo.** 2012. Temporal patterns of nucleotide misincorporations and DNA fragmentation in ancient DNA. PLoS ONE *7*:e34131.
27. **Jónsson, H., A. Ginolhac, M. Schubert, P.L. Johnson, and L. Orlando.** 2013. mapDamage2.0: fast approximate Bayesian estimates of ancient DNA damage parameters. Bioinformatics *29*:1682-1684.
28. **Friedberg, E.C., G.C. Walker, and W. Siede.** 1995. DNA repair and mutagenesis. ASM Press, Washington, D.C.

Received 19 January 2015; accepted 05 May 2015.

Address correspondence to Hendrik Poinar, McMaster Ancient DNA Centre, 1280 Main St. West, Hamilton, ON, L8S4L8, Canada. E-mail: poinarh@mcmaster.ca